

# Self-referenced and single-ended method to measure Brillouin gain in monomode optical fibers

Vincent Lanticq,<sup>1,2,3,\*</sup> Shifeng Jiang,<sup>2</sup> Renaud Gabet,<sup>2</sup> Yves Jaouën,<sup>2</sup> Frédéric Taillade,<sup>3</sup>  
Gautier Moreau,<sup>1</sup> and Govind P. Agrawal<sup>4</sup>

<sup>1</sup>Electricité de France R&D, 6 quai Watier, Chatou, 78401, France

<sup>2</sup>Institut Télécom/Télécom-Paristech, 46 rue Barrault, Paris, 75013, France

<sup>3</sup>Laboratoire Central des Ponts et Chaussées, 57 boulevard Lefebvre, Paris, 75015, France

<sup>4</sup>Institute of Optics, University of Rochester, Rochester, New York 14627-0186, USA

\*Corresponding author: vincent.lanticq@telecom-paristech.fr

Received December 23, 2008; revised February 11, 2009; accepted February 14, 2009;  
posted February 25, 2009 (Doc. ID 105708); published March 24, 2009

We present a new self-referenced and single-ended method to measure the Brillouin-gain coefficient in monomode optical fibers accurately with high reliability. Our comparative measurements on several different fibers show that a fiber with a smaller optical effective mode area can nevertheless have a higher Brillouin threshold, thus confirming the significance of acousto-optic effective mode area. © 2009 Optical Society of America

OCIS codes: 190.4370, 290.5830, 060.2270.

Stimulated Brillouin scattering (SBS) has remained an intensive research topic for many years [1]. The initial focus was on managing optical power limitations induced by SBS in optical fiber transmission systems and high-power fiber lasers. More recently, SBS properties have been exploited for numerous applications such as slow light, Brillouin fiber-ring lasers, and distributed fiber sensors. The Brillouin gain coefficient  $g_B$ , value of the Brillouin gain  $g(v)$  at the Brillouin frequency shift  $\nu_B$ , is the parameter usually chosen to describe the fiber sensitivity to SBS. However, a more appropriate parameter to describe SBS in monomode optical fibers would be  $C_B$ , value of  $C(v) = g(v)/A_{\text{eff}}^{\text{ao}}$  at frequency  $\nu_B$ ,  $A_{\text{eff}}^{\text{ao}}$  being the acousto-optic effective area defined by Eq. (11) of [2]. Indeed, according to amplified spontaneous Brillouin scattering theory,  $C_B$  is directly measurable and allows us to redefine the Brillouin threshold unambiguously by  $P_{th}C_B L \approx 21$  (where  $P_{th}$  is the pump power and fiber length is  $L = 100$  m [3]), without using either  $A_{\text{eff}}^{\text{ao}}$  or the optical effective area  $A_{\text{eff}}^o$ .

To measure  $C_B$  accurately, we have developed a new experimental technique based on the heterodyne detection of the amplified spontaneous Brillouin backscattering. Unlike the other accurate existing methods [4,5], this one is single ended: it requires access to only one end of the fiber. Even for spans shorter than 100 m, we have been able to determine the coefficient  $C_B$  with a relative uncertainty of better than 2%. In addition, our experiments reveal that  $C_B$  for a LEAF fiber can be two times smaller than that for a SMF28 fiber. These new measurements provide a clear example of what was claimed in [2]: *the decisive fiber parameter to quantify SBS is not the optical effective mode area but the acousto-optic interaction area.*

Before presenting our experimental data, we first re-express the theory briefly exposed in [6] using  $C_B$  instead of  $g_B$ . As in spontaneous Raman scattering theory, if an incident wave (the so-called pump wave) at the frequency  $\nu_0$  propagates along the  $z$  axis inside

an optical fiber (tens of meters long to cause significant differential group delay), backscattered photon numbers for the Stokes and anti-Stokes waves ( $N_S$  and  $N_{AS}$ ) can be determined, as a function of frequency shift  $\nu$ , by the following two equations (neglecting linear losses:  $L < 1$  km):

$$-\frac{dN_S}{dz} = \frac{1}{2}C(v)P_P(z)N_S(\nu_0 - \nu) + \frac{1 + \bar{n}}{2}C(v)P_P(z), \quad (1a)$$

$$-\frac{dN_{AS}}{dz} = -\frac{1}{2}C(v)P_P(z)N_{AS}(\nu_0 + \nu) + \frac{\bar{n}}{2}C(v)P_P(z), \quad (1b)$$

where  $P_P(z)$  is the pump power at a distance  $z$  and  $\bar{n}$  is the average thermal phonon number ( $\bar{n} \approx 600$  at  $\nu = 10$  GHz). We have assumed in Eq. (1) that the random nature of fiber birefringence creates an average coupling ratio of 1/2 between the pump and the backscattered signal. This would yield an unpolarized signal, in agreement with the experiments at low pump powers. Assuming  $P_P(0)$  is far from the power threshold ( $P_P L C_B < 10$ ), we neglect pump depletion and replace  $P_P(z)$  with the input pump power  $P_0$ , resulting in the following expressions for the Stokes and anti-Stokes photon numbers at the fiber input end at  $z = 0$ :

$$N_S(\nu_0 - \nu) = (1 + \bar{n}) \left[ \exp\left(\frac{1}{2}C(v)P_0 L\right) - 1 \right], \quad (2a)$$

$$N_{AS}(\nu_0 + \nu) = \bar{n} \left[ 1 - \exp\left(-\frac{1}{2}C(v)P_0 L\right) \right]. \quad (2b)$$

A simple self-heterodyne scheme (without the frequency shifter in Fig. 1) can be used to measure amplified spontaneous Brillouin scattering spectrum in the electrical domain, exactly as in [7]. Here, we add

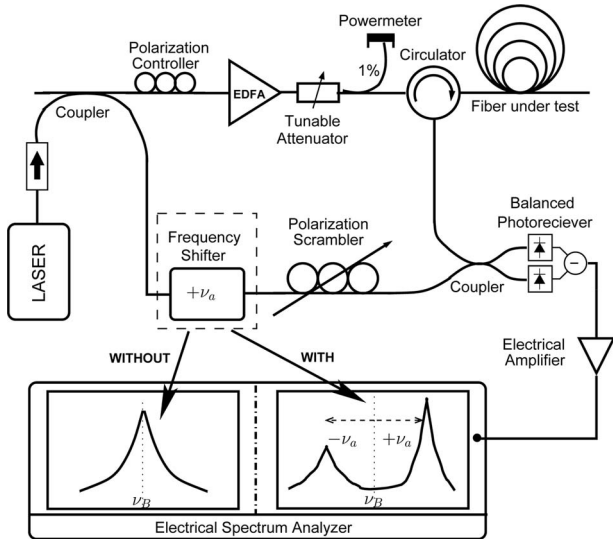


Fig. 1. Experimental setup used for measuring the Brillouin gain coefficient. The two insets marked WITHOUT and WITH show PSD changes produced by the frequency shifter.

a polarization scrambler to make our experiment polarization insensitive and restrict the error due to the unpolarized signal assumption made in the model (1). This feature was checked, even at a pump power higher than 0.5 W, by varying the state of polarization of the pump with a polarization controller located in the pump path. Further experiments and theoretical investigations are in progress to evaluate precisely this error as a function of  $P_0$ ,  $L$ ,  $C_B$ , and birefringence.

As shown in Fig. 1 (case WITHOUT), without the frequency shifter, power spectral densities (PSDs) of the detected Stokes and anti-Stokes signals overlap in the electrical domain. Nevertheless, since  $\bar{n} \gg 1$ , we can, in principle, measure  $C_B = C(\nu_B)$  from the total PSD corresponding to the maximum value of the Brillouin gain  $C(\nu)$ , because  $C(\nu)$  has a Lorentzian spectrum centered at  $\nu_B$ . The resulting expression for PSD is

$$\begin{aligned} \text{PSD}_{\text{elec}}(\nu) &= \gamma [N_{AS}(\nu_0 + \nu) + N_S(\nu_0 - \nu)] \\ &\approx 2\gamma\bar{n} \sinh\left(\frac{1}{2}C(\nu)P_0L\right), \end{aligned} \quad (3)$$

where  $\gamma$  is the transfer-function gain of the experimental setup and depends on factors such as photoreceiver sensitivity, optical losses, etc. Note, however, that an accurate determination of  $C_B$  requires a precise knowledge of the  $\gamma$  parameter, not an easy task. Moreover,  $\gamma$  could vary during measurements with extrinsic conditions, thereby limiting the measurement accuracy severely.

Here, we show that a  $\gamma$ -independent measurement of  $C_B$  can be performed with a simple modification of the self-heterodyne scheme. By inserting an acousto-optic modulator (shown as a dashed box in Fig. 1), acting as frequency upshifter, we can separate the Stokes and anti-Stokes PSDs in the electrical domain (see the case WITH). This frequency shifter can be in-

serted along any path of the heterodyne scheme. In our experiment, we chose to add this device in the local oscillator (LO) path, and set the frequency shift at  $\nu_a = 111$  MHz. As a result, the Stokes and anti-Stokes spectra were separated by an amount of  $2\nu_a = 222$  MHz in the electrical spectrum (see the case WITH). Since the Brillouin linewidth is about  $\Delta\nu_B = 40$  MHz for the fibers tested in our experiment, the two spectra are fully separated. For broader Brillouin spectra for which Stokes and anti-Stokes parts would overlap, larger values of  $\nu_a$  (or several modulators in series) could be used to separate them. For all fibers tested in this Letter, we measure simultaneously the maxima of both the Stokes and anti-Stokes PSDs. Unlike the previous case ( $\nu_a = 0$ ), where we were forced to use their sum, we can now calculate their ratio,

$$\frac{\text{PSD}_{\text{elec}}(\nu + \nu_a)}{\text{PSD}_{\text{elec}}(\nu - \nu_a)} = \frac{N_S(\nu_0 - \nu)}{N_{AS}(\nu_0 + \nu)} \approx \exp\left(\frac{1}{2}C(\nu)P_0L\right), \quad (4)$$

which is independent of the transfer-function gain  $\gamma$ . For this reason, we claim such a measurement to be self-referenced. Clearly, this feature ensures high reliability in the determination of  $C_B$ . From the PSD ratio, we define a parameter  $Y_C$  that depends on the pump power linearly,

$$Y_C = \frac{2}{L} \ln\left(\frac{\text{PSD}(\nu_B + \nu_a)}{\text{PSD}(\nu_B - \nu_a)}\right) = C_B P_0. \quad (5)$$

Our experimental procedure consists of plotting electrical PSDs and determining  $Y_C$  for several pump powers. Finally  $C_B$  is calculated by linear fit of the  $Y_C(P_0)$  curve. If the value of pump power injected into the fiber is known with sufficient accuracy, one could also evaluate  $C_B$  directly using only one pump power and calculating  $C_B = Y_C/P_0$ .

To validate the procedure described above, we first used our experimental setup to observe the separation of Stokes and anti-Stokes PSDs for a 65-m-long span of Corning SMF28 fiber, and the results are

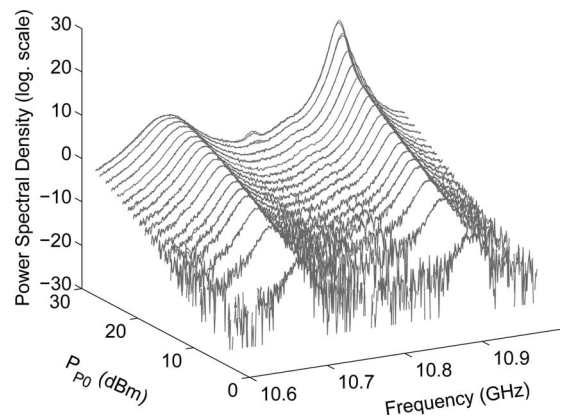


Fig. 2. Measured electrical power spectral density of a SMF28 fiber ( $L = 65$  m) for several pump powers. The Stokes spectrum is on the right and anti-Stokes on the left, owing to a frequency upshift in the LO path.

shown in Fig. 2 for several pump powers. As expected, the Stokes PSD is centered at  $\nu_B + \nu_a$  and the anti-Stokes one at  $\nu_B - \nu_a$ , and they are fully separated. In addition, both PSDs change with increasing pump power, as predicted by Eqs. (2). Indeed, our measurements are in full agreement with the theoretical predictions. From the PSD curves, we extract the maximum values of Stokes and anti-Stokes PSDs with a simple peak detection method. We used Eqs. (2) to fit our data [assuming  $C(v)$  has a Lorentzian shape] and determined the ratio of the PSD maxima and the value of  $Y_C$  as a function of the pump power  $P_0$ . Figure 3 shows the resulting linear plot from which we found  $C_B^{\text{SMF28}} = 0.195 \text{ m}^{-1} \text{ W}^{-1}$ . The relative uncertainty of our procedure is estimated to be within 2% by repeating the whole procedure on the same fiber span several times (fitting  $Y_C$  for 12 different pump powers  $P_0$ ). Assuming an acousto-optic effective area of  $A_{\text{SMF28}}^{\text{ao}} = 87 \text{ } \mu\text{m}^2$  (computed from [8]), this  $C_B$  value leads to  $g_B = 1.68 \times 10^{-11} \text{ mW}^{-1}$ . The values reported in literature range from  $g_B = 1.3 \times 10^{-11} \text{ mW}^{-1}$  [9] to  $g_B = 2.6 \times 10^{-11} \text{ mW}^{-1}$  [10,11] and are measured using different techniques such as a pump-probe method or changes in the Brillouin linewidth with pump power.

To study how the fiber design affects  $C_B$ , we used our method for two different spans of Corning LEAF fiber with lengths of 11.3 and 103 m. The measured  $Y_C$  as a function of  $P_0$  is also plotted in Fig. 3. The measured value of  $C_B^{\text{LEAF}} = 0.108 \text{ m}^{-1} \text{ W}^{-1}$  is the same for both spans. Indeed, Fig. 3 shows that  $Y_C$  varies identically in both cases, confirming that our measurement of  $C_B$  is length independent and can be made on spans as short as 11 m [if fiber birefringence is large enough to comply with Eqs. (1)].

The important point to note is that the  $C_B$  value of the LEAF fiber is lower (i.e., its Brillouin threshold is higher) than that of the SMF28 fiber, even though the optical effective area is smaller for the LEAF ( $A_{\text{LEAF}}^{\text{o}} \approx 70 \text{ } \mu\text{m}^2$  for LEAF fiber and  $A_{\text{SMF28}}^{\text{o}} \approx 80 \text{ } \mu\text{m}^2$  for SMF28). This is possible only if the relevant effective

area is not optical but the acousto-optic one is [2]. To verify that this is indeed the case, we estimated  $A_{\text{eff}}^{\text{ao}}$  for our LEAF fiber numerically and found a value around  $A_{\text{LEAF}}^{\text{ao}} \approx 160 \text{ } \mu\text{m}^2$  using [8] (we cannot provide a very accurate value, because the specific dopant profile for this fiber is not precisely known), which is more than twice the  $A_{\text{LEAF}}^{\text{o}}$  value. Using it, we find that the  $g_B$  value is almost the same for both the LEAF and SMF28 fibers. This is consistent with the common hypothesis that  $g_B$  is mainly intrinsic to the material [1]. Indeed, since both LEAF and SMF28 are weakly doped core fibers, there is no reason for fiber parameters to be very different for them. Our measurements highlight experimentally the fact, first demonstrated by [2], that the decisive parameter quantifying SBS in an optical fiber is not the optical effective area  $A_{\text{eff}}^{\text{o}}$  (that is relevant for the Kerr effect) but the acousto-optic interaction area  $A_{\text{eff}}^{\text{ao}}$ .

In summary, we proposed a new self-referenced, single-ended method to measure the Brillouin gain coefficient  $C_B$  for several fibers of different lengths (as short as 10 m) with a relative uncertainty of better than 2%, never before reached to the best of our knowledge. We found  $C_B^{\text{SMF28}} = 0.195 \text{ m}^{-1} \text{ W}^{-1}$  for a SMF28 fiber and  $C_B^{\text{LEAF}} = 0.108 \text{ m}^{-1} \text{ W}^{-1}$  for a LEAF fiber. We confirmed that optical effective area does not directly affect Brillouin scattering. In addition, the deduced  $g_B$  value varied slightly from one fiber to the other, indicating that the Brillouin gain parameter  $C_B$ , and thus the Brillouin threshold, are mainly affected by the acousto-optic effective area  $A_{\text{eff}}^{\text{ao}}$  of a fiber.

## References

1. G. P. Agrawal, *Nonlinear Fiber Optics*, 4th ed. (Academic, 2007).
2. A. Kobayakov, S. Kumar, D. Chowdhury, A. B. Ruffin, M. Sauer, S. Bickham, and R. Mishra, *Opt. Express* **15**, 5338 (2005).
3. S. Le Floch and P. Cambon, *J. Opt. Soc. Am. A* **20**, 1132 (2003).
4. A. Loayssa, R. Hernández, D. Benito, and S. Galech, *Opt. Lett.* **29**, 638 (2004).
5. A. Boh Ruffin, M.-J. Li, X. Chen, A. Kobayakov, and F. Annunziata, *Opt. Lett.* **30**, 3123 (2005).
6. V. Lanticq, S. Jiang, R. Gabet, Y. Jaouën, S. Delépine-Lesoille, and J. M. Hénault, in *Proceedings of the 34th European Conference on Optical Communication* (2008), paper Tu3.B.2.
7. A. Yeniay, J.-M. Delavaux, and J. Toulouse, *J. Lightwave Technol.* **20**, 1425 (2002).
8. V. Lanticq, R. Gabet, J.-L. Auguste, S. Delépine-Lesoille, S. Fortier, and Y. Jaouën, in *Proceedings of the 33rd European Conference on Optical Communication* (SPIE, 2007), paper WeP004.
9. C. Juregui Misas, P. Petropoulos, and D. J. Richardson, *J. Lightwave Technol.* **25**, 216 (2007).
10. M. Niklès, L. Thévenaz, and P. A. Robert, *J. Lightwave Technol.* **15**, 1842 (1997).
11. G. Canat, A. Durécu, G. Lesueur, L. Lombard, P. Bourdon, V. Jolivet, and Y. Jaouën, *Opt. Express* **16**, 3212 (2008).

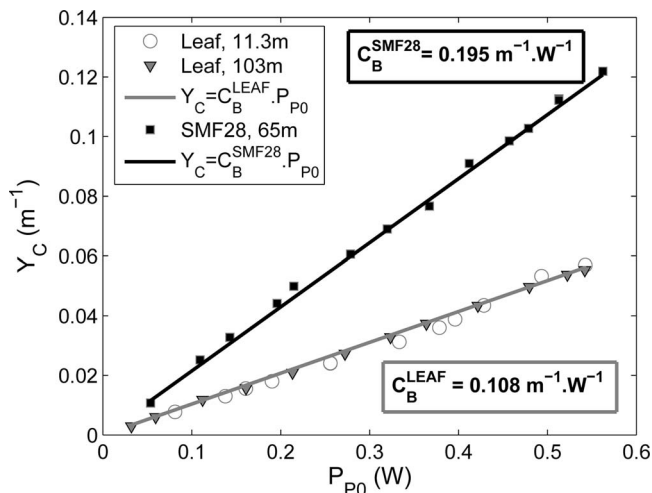


Fig. 3.  $Y_C$  as a function of pump power for the SMF28 fiber and two LEAF fibers of lengths indicated. Linear fits to data provide directly the values of  $C_B$ .